

# Associated Charmonium Production in Low Energy $p\bar{p}$ Annihilation

T.Barnes<sup>a,b\*</sup> and X.Li<sup>b†</sup>

<sup>a</sup>*Physics Division, Oak Ridge National Laboratory, Oak Ridge, TN 37831, USA*

<sup>b</sup>*Department of Physics and Astronomy, University of Tennessee, Knoxville, TN 37996, USA*

The QCD mechanisms underlying the exclusive strong decays and hadronic production amplitudes of charmonium remain poorly understood, despite decades of study and an increasingly detailed body of experimental information. One set of hadronic channels of special interest are those that include baryon-antibaryon states. These are being investigated experimentally at BES and CLEO-c in terms of their baryon resonance content, and are also of interest for the future PANDA experiment, in which charmonium and charmonium hybrids will be produced in  $p\bar{p}$  annihilation in association with light mesons. In this paper we develop a simple initial-state light meson emission model of the near-threshold associated charmonium production processes  $p\bar{p} \rightarrow \pi^0 \Psi$ , and evaluate the differential and total cross sections for these reactions in this model. (Here we consider the states  $\Psi = \eta_c, J/\psi, \psi', \chi_0$  and  $\chi_1$ .) The predicted near-threshold cross section for  $p\bar{p} \rightarrow \pi^0 J/\psi$  is found to be numerically similar to two previous theoretical estimates, and is roughly comparable to the (sparse) existing data for this process. The theoretical charmonium angular distributions predicted by this model are far from isotropic, which may be of interest for PANDA detector design studies.

PACS numbers: 11.80.-m, 13.60.Le, 13.75.Cs, 14.40.Gx

## I. INTRODUCTION

Strong decays of charmonia through annihilation of the  $c\bar{c}$  pair to light hadrons dominate the total widths of the lighter charmonium states [1]. In contrast to the faster open-charm decays, which appear to be reasonably well described by both the  $^3P_0$  model [2] and the Cornell timelike vector decay model [3] (given the current state of the data), the  $c\bar{c}$  annihilation decays are much less well understood. There are several general rules that appear to be respected by these decays; in particular, the number of QCD vertices in the leading-order Feynman diagram for annihilation into light quarks and gluons is a useful guide. For example, the  $C = (+)$  charmonia that can annihilate at  $O(g^2)$  (into  $gg$  for  $\eta_c, \chi_0, \chi_2$ , and  $q\bar{q}g$  for the  $\chi_1$ ) have strong annihilation widths of  $\sim 1 - 25$  MeV, often much larger than the  $\sim 0.1 - 0.3$  MeV widths of the  $C = (-)$  states  $J/\psi$  and  $\psi'$ , which must annihilate at  $O(g^3)$  into  $ggg$ . Since  $c\bar{c}$  annihilation is a short-ranged process (the charm quark propagator implies a range of  $r \sim 1/m_c$ ), a strong suppression of annihilation widths with increasing orbital angular momentum  $L_{c\bar{c}}$  is also anticipated; this suggests for example that the D-wave  $c\bar{c}$  states  $^1D_2$  and  $^3D_2$ , if below their  $DD^*$  open-charm threshold, will have strong widths of  $< 1$  MeV [3, 4].

Although the inclusive annihilation decays are qualitatively understood in terms of  $c\bar{c}$  annihilation into gluons, exclusive  $c\bar{c}$  annihilation decays remain a mystery, despite the existence of considerable experimental information on the branching fractions of some  $c\bar{c}$  states into specific exclusive modes. In particular, much is known about the exclusive two-body annihilation decays of the

$J/\psi$  and  $\psi'$ , and a “12% rule” for the relative branching fractions of the  $\psi'$  and  $J/\psi$  into many of these modes is part of charmonium folklore. The recent increase in the number of modes studied, for example by CLEO-c [5], has made it clear however that this rule is not generally applicable.

In this paper we note that there may be a simple relation between some two-body and three-body annihilation decays of charmonia, specifically in decays to the final states  $p\bar{p}$  and  $p\bar{p}\pi^0$ . These decays are of interest both as a novel technique for studying  $N^*$  spectroscopy, for example at BES [6, 7, 8, 9] and because they can be used to estimate the cross sections for associated charmonium production in  $p\bar{p}$  annihilation, as in  $p\bar{p} \rightarrow \pi^0 + \Psi$  [10]. (We use  $\Psi$  to represent a generic charmonium state.) These cross sections are of particular interest in that they will be exploited by the PANDA project at GSI [11] to search for excited charmonia and charmonium hybrids. The scales of these cross sections are at present largely unknown; a better understanding of these associated charmonium production processes near threshold is obviously crucial for planning various aspects of this experiment, such as detector design and data acquisition.

## II. THE MODEL

### A. Motivation

Since strong decays to three-body final states are typically dominated by quasi-two-body transitions, one might anticipate that decays of the type  $\Psi \rightarrow p\bar{p}\pi^0$  could be described as two-step processes,  $\Psi \rightarrow (N^{*+}\bar{p} + h.c.) \rightarrow p\bar{p}\pi^0$ , where the important  $N^*$  baryon isobars are those with large  $N\pi$  couplings. Specifically we might expect the nucleon itself to make a large or perhaps dominant contribution, in view of the large  $NN\pi$  coupling. This in

\*Email: tbarnes@utk.edu

†Email: xli22@utk.edu

turn suggests that the associated production of a  $\Psi$  state and a pion in  $p\bar{p}$  annihilation may take place through initial emission of a pion from the incoming  $p$  or  $\bar{p}$  line, followed by direct annihilation of the  $p\bar{p}$  state into  $c\bar{c}$ . At tree level this process is described by the two Feynman diagrams of Fig.1.

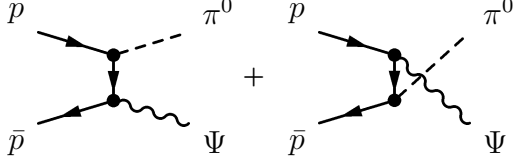


FIG. 1: Feynman diagrams assumed in this model of the generic reaction  $p\bar{p} \rightarrow \pi^0 \Psi$ .

The use of these simple hadron-level “pole” diagrams to describe these processes was previously suggested by Gaillard, Maiani and Petronzio [12], who considered the production of charmonium from  $p\bar{p}$  states with specified initial quantum numbers. Their work was subsequently extended analytically by Lundborg, Barnes and Wiedner [10] (much of Ref.[12] was numerical). Lundborg *et al.* also showed that a constant amplitude approximation could be used to estimate the cross section for  $p\bar{p} \rightarrow \pi^0 \Psi$  from the corresponding three-body decay  $\Psi \rightarrow p\bar{p}\pi^0$ ; numerical results for  $\sigma(p\bar{p} \rightarrow \pi^0 J/\psi)$  using both approaches are given in that reference.

The work presented here gives extensive analytic results for differential and total cross sections derived from the pole model, assuming plane wave initial  $p\bar{p}$  states. If the partial width of a charmonium state  $\Psi$  to  $p\bar{p}$  is known experimentally, one can use this to estimate the corresponding  $\Psi - p\bar{p}$  coupling constant  $g_{p\bar{p}\Psi}$ . Since the  $NN\pi$  coupling constant is known, one may then evaluate the differential and total cross sections for  $p\bar{p} \rightarrow \pi^0 \Psi$  both analytically and numerically in this model. Here we carry out this exercise for the cases of five low-lying  $\Psi$  states with known  $p\bar{p}$  partial widths, specifically the  $\eta_c, J/\psi, \psi', \chi_0$  and  $\chi_1$ .

## B. Amplitudes

We describe the reactions  $p\bar{p} \rightarrow \pi^0 \Psi$  as two step processes, initial pion emission from an incident proton or antiproton followed by direct annihilation of the proton-antiproton pair,  $p\bar{p} \rightarrow \Psi$ . This process at tree level is described by the two Feynman diagrams of Fig.1. The  $p\bar{p}\pi^0$  and  $\bar{p}p\pi^0$  vertices are taken to be the usual  $g_{pp\pi}\gamma_5$ , and the  $p\bar{p}\Psi$  vertex is generically  $g_{p\bar{p}\Psi}\Gamma$ , where the Dirac matrix  $\Gamma$  specifies the quantum numbers of the state  $\Psi$ . We use  $\Gamma = \gamma_5$  for the  $\eta_c$ ,  $-i$  for the  $\chi_0$ ,  $-i\gamma_\mu$  for the  $J/\psi$  and  $\psi'$ , and  $-i\gamma_\mu\gamma_5$  for the  $\chi_1$ . For the vector and axial-vector cases  $J/\psi, \psi'$  and  $\chi_1$ ,  $\Gamma$  is implicitly contracted into the final  $\Psi$  polarization four-vector  $\epsilon_\mu^*$ .

The resulting invariant amplitude is

$$\mathcal{M} = ig_\pi g_\Psi \bar{v}_{\bar{p}s} \left[ \Gamma \frac{(\not{p} - \not{k} + m)}{(t - m^2)} \gamma_5 + \gamma_5 \frac{(\not{k} - \not{p} + m)}{(u - m^2)} \Gamma \right] u_{ps}. \quad (1)$$

Here and in the following expressions  $m$  is the proton mass,  $m_\pi$  is the pion mass,  $M$  is the mass of the charmonium state  $\Psi$ , and  $r_\pi = m_\pi/m$  and  $r_\Psi = M/m$  are dimensionless mass ratios relative to the proton. The pion-nucleon coupling constant is  $g_\pi \equiv g_{pp\pi}$ , and the (state-dependent) charmonium- $p\bar{p}$  coupling constant is  $g_\Psi \equiv g_{p\bar{p}\Psi}$ . We also define squared strong coupling constants  $\alpha_\pi \equiv g_{pp\pi}^2/4\pi$  and  $\alpha_\Psi \equiv g_{p\bar{p}\Psi}^2/4\pi$ .

It is sometimes useful to rewrite this invariant amplitude in an equivalent form that makes the overall  $t \leftrightarrow u$  crossing symmetry more evident;

$$\mathcal{M} = -\frac{ig_\pi g_\Psi/2}{(t - m^2)(u - m^2)}.$$

$$\left[ (s - M^2 - m_\pi^2) \bar{v}_{\bar{p}s} \{ \gamma_5 \not{k}, \Gamma \} u_{ps} - (t - u) \bar{v}_{\bar{p}s} [ \gamma_5 \not{k}, \Gamma ] u_{ps} \right]. \quad (2)$$

Since the commutator (anticommutator) of  $\gamma_5 \not{k}$  with  $\Gamma$  vanishes for scalar (pseudoscalar)  $\Psi$ , this rearrangement simplifies the calculation considerably in these cases.

## C. Massless pions

### 1. Differential cross sections

The differential and total cross sections we find given this invariant amplitude are rather simple in the massless pion limit, and only involve two independent functions. For this reason we first give results for massless pions, and then treat each set of charmonium quantum numbers separately for nonzero pion mass. Our results for the unpolarized differential cross sections in the massless pion limit are

$$\left\langle \frac{d\sigma}{dt} \right\rangle \Big|_{p\bar{p} \rightarrow \pi^0 \eta_c} = \frac{\pi}{2} \frac{\alpha_\pi \alpha_\Psi}{s(s - 4m^2)} \frac{(x - y)^2}{xy}, \quad (3)$$

$$\left\langle \frac{d\sigma}{dt} \right\rangle \Big|_{p\bar{p} \rightarrow \pi^0 \chi_0} = \frac{1}{2} \left\langle \frac{d\sigma}{dt} \right\rangle \Big|_{p\bar{p} \rightarrow \pi^0 (J/\psi, \psi')} = \frac{\pi}{2} \frac{\alpha_\pi \alpha_\Psi}{s(s - 4m^2)} \frac{f^2}{xy}, \quad (4)$$

$$\left\langle \frac{d\sigma}{dt} \right\rangle \Big|_{p\bar{p} \rightarrow \pi^0 \chi_1} = \pi \frac{\alpha_\pi \alpha_\Psi}{s(s - 4m^2)} \cdot \left[ \left( 1 - 2/r_\Psi^2 \right) \frac{f^2}{xy} + 2(r_\Psi^2 f - 1) \right]. \quad (5)$$

Here  $x$  and  $y$  are dimensionless, shifted Mandelstam variables  $x \equiv t/m^2 - 1$  and  $y \equiv u/m^2 - 1$ , and  $f$  is a dimensionless energy variable, which for general masses is given by  $f = (s - m_\pi^2 - M^2)/m^2 = -(x + y)$ .

There are several interesting features in these angular distributions which are relevant to PANDA. Note that the differential cross sections in Eqs.(3-5) are  $t \leftrightarrow u$  ( $x \leftrightarrow y$ ) crossing symmetric, and that there are maxima in the forward and backwards directions, which give the largest values for the proton propagator functions  $1/|t - m^2| = 1/m^2|x|$  and  $1/|u - m^2| = 1/m^2|y|$ . A more striking effect is the zero in the angular distribution of the final state  $\pi^0\eta_c$ , which follows from the odd  $t \leftrightarrow u$  spatial symmetry of this amplitude; this implies a node at  $t = u$ , corresponding to  $\theta = \pi/2$  in the  $c.m.$  frame. In comparison the angular distributions of the other final states we consider also have minima at  $t = u$ , but are nonzero there. These rapidly varying angular distribution could be used to test for the presence of this signal over the presumably more slowly varying backgrounds.

## 2. Total cross sections

In the massless pion limit the unpolarized total cross sections follow from integrating the results in Eqs.(3-5) over  $t$ . They may conveniently be written as functions of  $s$  and  $\beta = \sqrt{1 - 4m^2/s}$  (the  $p$  or  $\bar{p}$  velocity in the  $c.m.$  frame), and are given by

$$\langle\sigma\rangle\Big|_{p\bar{p}\rightarrow\pi^0\eta_c} = 2\pi\alpha_\pi\alpha_\Psi \frac{(s - M^2)}{s^2\beta^2} \left[ \tanh^{-1}\beta - \beta \right] \quad (6)$$

$$\langle\sigma\rangle\Big|_{p\bar{p}\rightarrow\pi^0\chi_0} = 2\pi\alpha_\pi\alpha_\Psi \frac{(s - M^2)}{s^2\beta^2} \tanh^{-1}\beta \quad (7)$$

$$\langle\sigma\rangle\Big|_{p\bar{p}\rightarrow\pi^0\chi_1} = 2\pi\alpha_\pi\alpha_\Psi \frac{(s - M^2)}{s^2\beta^2} \cdot \left[ 2(1 - 2/r_\Psi^2) \tanh^{-1}\beta + (s/M^2 - 2)\beta \right]. \quad (8)$$

The massless pion total cross section formulas for the final states  $\pi^0 J/\psi$  and  $\pi^0\psi'$  are proportional to the  $\pi^0\chi_0$  result, as implied by Eq.(4);  $\sigma(J/\psi) = \sigma(\psi') = 2\sigma(\chi_0)$ . We stress that these simple ratios only apply to the algebraic expressions; the actual numerical cross sections are not simply related, due to *a)* different kinematics, and *b)* the strongly state-dependent  $g_{p\bar{p}\Psi}$  couplings, which are given in Table I.

## D. Massive pions

### 1. Kinematics

The results given in the previous section for massless pions are attractive in their simplicity, and are useful

for numerical estimates well above threshold. However we find that the angular distributions near threshold are strongly dependent on the pion mass (the massless case is a singular limit), and the difference in the location of the threshold for massless versus massive pions leads to numerically important differences in the predicted cross sections at energies relevant to PANDA. For these reasons we give detailed predictions for the differential and total cross sections for these charmonium production processes in the case of general pion mass.

Since we will discuss some angular distributions in the  $c.m.$  frame, it is useful to have the relation between Mandelstam variables and proton ( $p$ ) and pion ( $k$ ) variables in this frame for general masses. These relations are

$$E_p = \frac{s^{1/2}}{2} \quad (9)$$

$$p = \frac{s^{1/2}}{2} \left( 1 - \frac{4m^2}{s} \right)^{1/2} \quad (10)$$

$$E_k = \frac{s^{1/2}}{2} \left( 1 - \frac{(M^2 - m_\pi^2)}{s} \right) \quad (11)$$

$$k = \frac{s^{1/2}}{2} \left( 1 - \frac{2(M^2 + m_\pi^2)}{s} + \frac{(M^2 - m_\pi^2)^2}{s^2} \right)^{1/2} \quad (12)$$

### 2. Differential cross sections

For general pion mass the differential cross sections  $\{\langle d\sigma/dt \rangle\}$  may be written as multiplier functions  $\{F_\Psi\}$  times the massless pion formulas of Eqs.(3-5). These functions, expressed as power series in  $r_\pi = m_\pi/m$ , are

$$F_{\eta_c} = 1 - \frac{r_\Psi^2}{xy} r_\pi^2 \quad (13)$$

$$F_{\chi_0} = 1 - \frac{(r_\Psi^2 - 4)}{xy} r_\pi^2 \quad (14)$$

$$F_{J/\psi, \psi'} = 1 + \left( \frac{2(r_\Psi^2 + f)}{f^2} - \frac{(r_\Psi^2 + 2)}{xy} \right) r_\pi^2 + \frac{2}{f^2} r_\pi^4. \quad (15)$$

In the  $\chi_1$  case it is simpler to give the full differential cross section with nonzero pion mass directly. This result is

$$\begin{aligned} \left\langle \frac{d\sigma}{dt} \right\rangle\Big|_{p\bar{p}\rightarrow\pi^0\chi_1} &= \pi \frac{\alpha_\pi\alpha_\Psi}{s(s - 4m^2)} \cdot \\ &\left\{ \left[ 2(f/r_\Psi^2 - 1) + \frac{(1 - 2/r_\Psi^2)f^2}{xy} \right] \right. \\ &\left. + \left[ \frac{2}{r_\Psi^2} + \frac{2(r_\Psi^2 - f - 4)}{xy} - \frac{(r_\Psi^2 - 4)f^2}{(xy)^2} \right] r_\pi^2 - \frac{2}{xy} r_\pi^4 \right\}. \quad (16) \end{aligned}$$

Examples of these angular distributions will be shown in the section on numerical results.

### 3. Total cross sections

In the case of general masses, inspection of the differential cross sections implied by Eqs.(3-5) and Eqs.(13-16) shows that the total cross sections may all be evaluated analytically in terms of integrals over  $x$ , which are generically of the form

$$\mathcal{I}_m = \int_{x_0}^{x_1} \frac{dx}{(xy)^m} \quad (17)$$

where  $y = -x - f$ . The limits of integration are implied by the definition  $x = t/m^2 - 1$ , and in terms of proton ( $p$ ) and pion ( $k$ ) *c.m.* frame energies and three-momenta are

$$x_1 = (m_\pi^2 - 2E_p E_k \pm 2pk)/m^2. \quad (18)$$

These limits may also be written in terms of masses and the Mandelstam variable  $s$ , using the relations given in Eqs.(9-12). The explicit indefinite integrals required for our cross section calculations are

$$\mathcal{I}_0(x) = x \quad (19)$$

$$\mathcal{I}_1(x) = \frac{1}{f} \ln \left( \frac{x+f}{x} \right) \quad (20)$$

$$\mathcal{I}_2(x) = \frac{2}{f^3} \ln \left( \frac{x+f}{x} \right) - \frac{1}{f^2} \left( \frac{1}{x+f} + \frac{1}{x} \right). \quad (21)$$

In terms of these integrals, evaluated between the limits  $x_0$  and  $x_1$  (so that  $\mathcal{I}_m \equiv \mathcal{I}_m(x_1) - \mathcal{I}_m(x_0)$ ), the total cross sections are

$$\langle \sigma \rangle_{p\bar{p} \rightarrow \pi^0 \eta_c} = \frac{\pi \alpha_\pi \alpha_\Psi}{2} \frac{m^2}{s(s-4m^2)} \cdot \left[ - (4\mathcal{I}_0 - f^2 \mathcal{I}_1) + r_\pi^2 r_\Psi^2 (4\mathcal{I}_1 - f^2 \mathcal{I}_2) \right] \quad (22)$$

$$\langle \sigma \rangle_{p\bar{p} \rightarrow \pi^0 (J/\psi, \psi')} = \pi \alpha_\pi \alpha_\Psi \frac{m^2}{s(s-4m^2)} \cdot \left[ f^2 \mathcal{I}_1 + r_\pi^2 (2(r_\Psi^2 + f) \mathcal{I}_1 - (r_\Psi^2 + 2) f^2 \mathcal{I}_2) + r_\pi^4 2\mathcal{I}_1 \right] \quad (23)$$

$$\langle \sigma \rangle_{p\bar{p} \rightarrow \pi^0 \chi_0} = \frac{\pi \alpha_\pi \alpha_\Psi}{2} \frac{m^2 f^2}{s(s-4m^2)} \left[ \mathcal{I}_1 - r_\pi^2 (r_\Psi^2 - 4) \mathcal{I}_2 \right] \quad (24)$$

$$\langle \sigma \rangle_{p\bar{p} \rightarrow \pi^0 \chi_1} = \pi \alpha_\pi \alpha_\Psi \frac{m^2}{s(s-4m^2)} \cdot \left[ \left( 2(f/r_\Psi^2 - 1) \mathcal{I}_0 + f^2 (1 - 2/r_\Psi^2) \mathcal{I}_1 \right) + r_\pi^2 \left( 2/r_\Psi^2 \mathcal{I}_0 + 2(r_\Psi^2 - f - 4) \mathcal{I}_1 - f^2 (r_\Psi^2 - 4) \mathcal{I}_2 \right) - r_\pi^4 2\mathcal{I}_1 \right]. \quad (25)$$

These cross sections will be evaluated numerically in the next section.

## III. NUMERICAL RESULTS

### A. Estimating the $p\bar{p}\Psi$ coupling constants

Numerical evaluation of our predictions for cross sections and related quantities requires values for the model parameters. The hadron masses are of course well known, as is the  $NN\pi$  coupling constant  $g_\pi \equiv g_{pp\pi}$ , which we take to be 13.5. The coupling strengths of the various charmonium resonances to  $p\bar{p}$  however are not well established; this is a crucial issue for the PANDA project, which assumes that these couplings are sufficiently large to allow the accumulation of large charmonium event samples in  $p\bar{p}$  annihilation.

Since the partial widths of several charmonium states to  $p\bar{p}$  are now known experimentally, one may estimate these state-dependent charmonium- $p\bar{p}$  coupling constants  $\{g_\Psi\}$  by equating the measured partial widths to the  $O(g_\Psi^2)$  theoretical partial widths we calculate in our model, assuming the same pointlike  $p\bar{p}\Psi$  vertices that we used to calculate the  $p\bar{p} \rightarrow \pi^0 \Psi$  cross sections. In terms of the  $\alpha_\Psi = g_{p\bar{p}\Psi}^2/4\pi$  and the final  $p$  velocity  $\beta = \sqrt{1 - 4m^2/M^2}$ , these partial widths are

$$\Gamma(\eta_c \rightarrow p\bar{p}) = \alpha_{\eta_c} \beta M/2 \quad (26)$$

$$\Gamma(J/\psi \rightarrow p\bar{p}) = \alpha_{J/\psi} \beta (1 + 2/r_\Psi^2) M/3 \quad (27)$$

$$\Gamma(\chi_0 \rightarrow p\bar{p}) = \alpha_{\chi_0} \beta^3 M/2 \quad (28)$$

$$\Gamma(\chi_1 \rightarrow p\bar{p}) = \alpha_{\chi_1} \beta^3 M/3. \quad (29)$$

We use these relations and the measured branching fractions and total widths to estimate values for the various charmonium- $p\bar{p}$  coupling constants; these results are shown in Table I. Note that the couplings of the pseudoscalar and scalar states  $\eta_c$  and  $\chi_0$  to  $p\bar{p}$  are an order of magnitude larger than the couplings of the vector and axial vector states.

State $\Psi$	$B_{\Psi \rightarrow p\bar{p}}$	$\Gamma_\Psi^{tot.} [\text{MeV}]$	$10^3 \cdot g_{p\bar{p}\Psi}$
$\eta_c$	$(1.3 \pm 0.4) \cdot 10^{-3}$	$25.5 \pm 3.4$	$19.0 \pm 3.2$
$J/\psi$	$(2.17 \pm 0.08) \cdot 10^{-3}$	$0.0934 \pm 0.0021$	$1.62 \pm 0.03$
$\psi'$	$(2.65 \pm 0.22) \cdot 10^{-4}$	$0.337 \pm 0.013$	$0.97 \pm 0.04$
$\chi_0$	$(2.24 \pm 0.27) \cdot 10^{-4}$	$10.4 \pm 0.7$	$5.42 \pm 0.37$
$\chi_1$	$(6.7 \pm 0.5) \cdot 10^{-5}$	$0.89 \pm 0.05$	$1.03 \pm 0.07$
$\chi_2$	$(6.6 \pm 0.5) \cdot 10^{-5}$	$2.06 \pm 0.12$	—

TABLE I: Charmonium- $p\bar{p}$  coupling constants, estimated from the measured branching fractions and total widths [1] and the  $\Gamma_{\Psi \rightarrow p\bar{p}}$  width formulas of Eqs.(26-29) (see text).

## B. Total Cross Sections

We will now evaluate the total unpolarized cross sections  $\langle\sigma\rangle(p\bar{p} \rightarrow \pi^0\Psi)$  for the five cases  $\Psi = \eta_c, J/\psi, \chi_0, \chi_1$  and  $\psi'$ , using the formulas given in Eqs.(22-25). The masses assumed are 2006 PDG values [1] rounded to 0.1 MeV;  $m_{\pi^0} = 0.1350$  GeV,  $m_p = 0.9383$  GeV  $M_{\eta_c} = 2.9804$  GeV,  $M_{J/\psi} = 3.0969$  GeV,  $M_{\chi_0} = 3.4148$  GeV,  $M_{\chi_1} = 3.5107$  GeV and  $M_{\psi'} = 3.6861$  GeV. The  $pp\pi^0$  coupling constant is taken to be  $g_\pi = 13.5$ , and the  $p\bar{p}\Psi$  couplings are given in Table I. The resulting cross sections are shown in Fig.2.

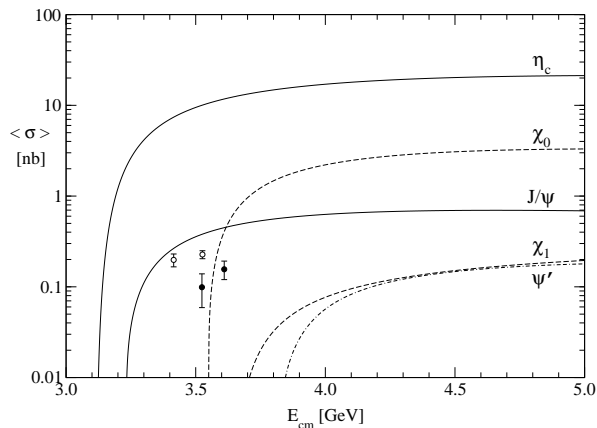


FIG. 2: Predicted unpolarized total cross sections for the processes  $p\bar{p} \rightarrow \pi^0\Psi$ , where  $\Psi = \eta_c, J/\psi, \chi_0, \chi_1$  and  $\psi'$ . The data points are Fermilab measurements of the cross section for  $p\bar{p} \rightarrow \pi^0 J/\psi$ , from E760 [13] (filled) and E835 [14] (open). There are additional experimental results for this reaction from E835 [15] which have not yet been published as a physical cross section.

Evidently these cross sections share a rapid rise above threshold, followed by a slowly varying “plateau” region above  $E_{cm} \approx 4$  GeV. The most remarkable feature may be the wide variation in the plateau values with the charmonium state  $\Psi$ . The largest cross section by far is for  $\eta_c$  production, which is roughly a factor of 30 larger than the  $J/\psi$  cross section. Second is the  $\chi_0$  cross section, roughly 5 times larger than  $J/\psi$ . Since the  $\chi_0$  has a radiative branching fraction to  $\gamma J/\psi$  of  $35.6 \pm 1.9\%$ , this implies that  $J/\psi$  production through the radiative process  $p\bar{p} \rightarrow \pi^0\chi_0, \chi_0 \rightarrow \gamma J/\psi$  is comparable to the direct process  $p\bar{p} \rightarrow \pi^0 J/\psi$ . Finally, the  $\chi_1$  and  $\psi'$  cross sections are smaller than the  $J/\psi$  by about a factor of 5-10. (For the  $\psi'$  to  $J/\psi$  ratio this is reminiscent of the 12% rule for a radial excitation.) These results suggest that the associated production of charmonium and charmonium hybrids with certain quantum numbers is strongly enhanced in  $p\bar{p}$  production, and that  $J^{PC} = 0^{-+}$  and  $0^{++}$  states may be the most favored.

## C. Angular distributions

The angular distributions predicted by this model of  $p\bar{p} \rightarrow \pi^0\Psi$  are especially interesting, since they are far from isotropic and may be important for design of the PANDA detector. Two representative cases for  $\langle d\sigma/d\Omega \rangle$  (*c.m.* frame) are shown in the figures; both show angular distributions normalized to unity in the forward direction, with  $E_{cm}$  in steps of 0.2 GeV up to a cutoff of  $E_{cm} = 5.0$  GeV. The contours at  $E_{cm} = 4.0$  GeV and  $E_{cm} = 5.0$  GeV are highlighted.

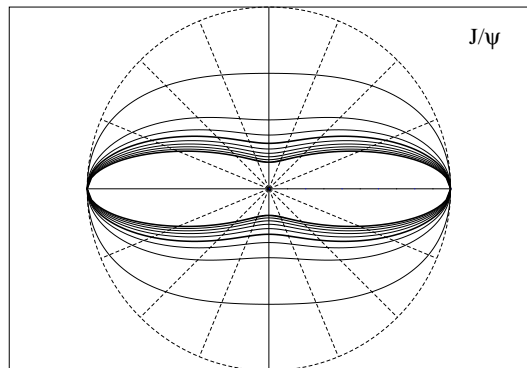


FIG. 3: Predicted *c.m.* frame unpolarized angular distribution  $\langle d\sigma/d\Omega \rangle$  for the process  $p\bar{p} \rightarrow \pi^0 J/\psi$ , normalized to the forward intensity, for  $E_{cm} = 3.4 - 5.0$  GeV in steps of 0.2 [GeV].

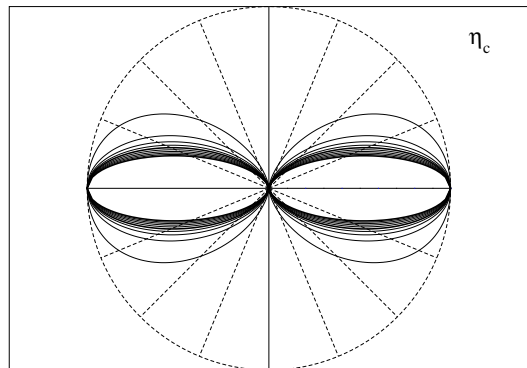


FIG. 4: The corresponding angular distribution for the reaction  $p\bar{p} \rightarrow \pi^0 \eta_c$ , for  $E_{cm} = 3.2 - 5.0$  GeV in steps of 0.2 [GeV].

The first angular distribution, in Fig.3, shows the prediction of Eqs.(4,15) for the reaction  $p\bar{p} \rightarrow \pi^0 J/\psi$ . This distribution is isotropic as we approach threshold, but with increasing  $E_{cm}$  evidently becomes strongly forward- and backward-peaked. (All the unpolarized cross sections we consider are front-back symmetric.)

The second angular distribution is for the reaction  $p\bar{p} \rightarrow \pi^0 \eta_c$ , which is predicted to be the largest associated charmonium production cross section by a considerable margin. This angular distribution, taken from

Eqs.(3,13), is shown in Fig.4. (The same conventions are used as in the previous figure.) This differential cross section shows a similar forward- and backward-peaking with increasing  $E_{cm}$ , and has in addition a very characteristic node at  $t = u$ , which is  $\theta = 90^\circ$  in the  $c.m.$  frame. The large overall scale of this cross section suggests that the detection of unusual modes such as  $p\bar{p} \rightarrow 4\gamma$  may be feasible (with both the  $\pi^0$  and  $\eta_c$  decaying to  $\gamma\gamma$ ).

#### IV. SUMMARY AND FUTURE

In this paper we have developed a hadronic “pole” model of charmonium production with an associated pion in proton-antiproton collisions. Given the Feynman diagrams of Fig.1 we derived closed-form analytic results for the unpolarized differential and total cross sections for the processes  $p\bar{p} \rightarrow \pi^0\Psi$ , where the quantum numbers considered for the charmonium state  $\Psi$  were  $0^{-+}, 0^{++}, 1^{--}$  and  $1^{++}$ . We quoted results for both massless and massive pions.

Besides the hadron masses this model has as free parameters the known  $g_{p\pi\pi^0}$  and the coupling  $g_{p\bar{p}\Psi}$  of the specified charmonium state  $\Psi$  to  $p\bar{p}$ . Here we used the experimental partial widths of light charmonium states to  $p\bar{p}$  to estimate the coupling constants  $\{g_{p\bar{p}\Psi}\}$ . Given this information we numerically evaluated the differential and total cross sections for these reactions. In particular we gave numerical predictions for the total cross section for the cases  $\Psi = \eta_c, J/\psi, \chi_0, \chi_1$  and  $\psi'$  (Fig.2), and for the differential cross sections in two representative cases,  $\Psi = J/\psi$  (Fig.3) and  $\eta_c$  (Fig.4). The two published data points from E760 for the  $p\bar{p} \rightarrow \pi^0 J/\psi$  total cross section near 3.5 GeV (Fig.2) suggest that our results overestimate the cross section at this  $E_{cm}$  by about a factor of 2.

The total cross sections predicted for the other reactions are especially interesting. The reaction  $p\bar{p} \rightarrow \pi^0\eta_c$  is predicted to have the largest cross section by a considerable margin, followed by the  $\chi_0$ . The two smallest cross sections are predicted for the  $\chi_1$  and  $\psi'$ . These results suggest that  $J^{PC} = 0^{-+}$  and  $0^{++}$  charmonium states

may be the most copiously produced in the PANDA experiment. A comparison of the  $J/\psi$  and  $\psi'$  suggests that the first radial excitation cross sections are suppressed relative to the ground states by about a factor of 5-10 in the relevant PANDA energy regime.

Several future developments related to this type of model appear especially interesting. The important question of the size of the associated production cross sections of other charmonium states can be answered in this model given their  $p\bar{p}$  branching fractions, so  $B_{p\bar{p}}$  is a very important measurements for the charmonium states we have not considered here. Similarly, the cross sections for emission of a charmonium state  $\Psi$  accompanied by other light mesons  $\{m\}$  can be studied; this may also be used to clarify poorly known  $ppm$  couplings. The importance of initial and final polarizations, which may be accessible at PANDA, can easily be addressed in this model. An important effect which has not been included is the contribution of intermediate  $N^*$  resonances to the  $p\bar{p} \rightarrow \pi^0\Psi$  transition amplitudes; the  $NN^*\Psi$  couplings can be extracted from the corresponding  $\Psi \rightarrow NN^*$  decays. Finally, as our approximation of pointlike hadron vertices is unrealistic well above threshold, it would be very interesting to study the effect of plausible  $pp\pi^0$  and  $p\bar{p}\Psi$  form factors on our results.

#### V. ACKNOWLEDGEMENTS

We are happy to acknowledge useful communications with D.Bettoni, C.Patrignani, T.Pedlar and K.Seth regarding experimental results for associated charmonium production cross sections at Fermilab. We also gratefully acknowledge support from K.Peters at GSI in Summer 2006, where this work was initiated. This research was supported in part by the U.S. National Science Foundation through grant NSF-PHY-0244786 at the University of Tennessee, and the U.S. Department of Energy under contract DE-AC05-00OR22725 at Oak Ridge National Laboratory.

- 
- [1] Review of Particle Physics, W.-M.Yao *et al.*, J. Phys. G33, 1 (2006).
  - [2] T. Barnes, S. Godfrey and E. S. Swanson, Phys. Rev. D **72**, 054026 (2005) [arXiv:hep-ph/0505002].
  - [3] E. J. Eichten, K. Lane and C. Quigg, Phys. Rev. D **69**, 094019 (2004) [arXiv:hep-ph/0401210].
  - [4] T. Barnes and S. Godfrey, Phys. Rev. D **69**, 054008 (2004) [arXiv:hep-ph/0311162].
  - [5] R. A. Briere *et al.* [CLEO-c Collaboration], arXiv:hep-ex/0505101.
  - [6] J. Z. Bai *et al.* [BES Collaboration], Phys. Lett. B **510**, 75 (2001) [arXiv:hep-ex/0105011].
  - [7] M. Ablikim *et al.* [BES Collaboration], arXiv:hep-ex/0405030.
  - [8] M. Ablikim *et al.* [BES Collaboration], arXiv:hep-ex/0503030.
  - [9] W. H. Liang, P. N. Shen, B. S. Zou and A. Faessler, Eur. Phys. J. A **21**, 487 (2004) [arXiv:nucl-th/0404024].
  - [10] A. Lundborg, T. Barnes and U. Wiedner, Phys. Rev. D **73**, 096003 (2006) [arXiv:hep-ph/0507166].
  - [11] Technical Progress Report for: PANDA, Strong Interaction Studies with Antiprotons (Feb. 2005).
  - [12] M. K. Gaillard, L. Maiani and R. Petronzio, Phys. Lett. B **110** (1982) 489.
  - [13] T. A. Armstrong *et al.*, Phys. Rev. Lett. **69**, 2337 (1992).
  - [14] D. N. Joffe, arXiv:hep-ex/0505007.
  - [15] M. Andreotti *et al.*, Phys. Rev. D **72**, 032001 (2005).